Navigation of an Autonomous Mobile Robot Using Data Association Method

Amir Monjazeb[1], Jurek Z. Sasiadek[1] and Dan Necsulescu[2]

[1]*Department of Mechanical and Aerospace Engineering, Carleton University, 1125 Colonel By Drive, Ottawa, Canada*
[2]*Department of Mechanical Engineering, Ottawa University, 161 Louis Pasteur, CBY A205, Ottawa, Canada*

Abstract: This paper presents an investigation on the performance of Unscented HybridSLAM using two different mapping strategies. The global map estimation using Unscented Kalman Filter is scrutinized for different scenarios, with and without the influence of a data association process. The accuracy of generated global map under different vehicle speed settings and with different process time is demonstrated using computer simulation. Results are discussed in terms of Root Mean Square (RMS) position error, orientation error, and time of navigation process. Results show that depending on the application, and on a desired speed, a compromise has to be done to get the best efficacy.

1 INTRODUCTION

Simultaneous Localization and Mapping (SLAM) problem is often implemented in autonomous mobile robots applications. SLAM is a situation in which a mobile robot steers in an unknown environment and constructs an instantaneous map and uses that map to localize. Once localized, the robot updates the map from its new location and this process occurs simultaneously and in consequent fragments of time (Durrant-Whyte, Bailey, 2006). SLAM was introduced about three decades ago in terms of uncertainty estimation of an erroneous dynamic Bayesian network (Smith, Cheesman, 1986). Since then, a continuous development of SLAM structure and different solutions to the problem were accomplished. Nowadays, SLAM is presented in two major categories; feature-based and location-based (Jaulin, 2011). This study focuses on some aspects of the feature-based SLAM which furthers the research on a new approach called Unscented HybridSLAM (UHS) (Monjazeb et al., 2013). The approach is combined of Unscented Kalman filter (Julier, Uhlmann, 2001) and FastSLAM (Montemerlo, et al., 2002) which is using the similar navigational strategies in HybridSLAM (HS) structure (Brooks, Bailey, 2009) and constrained local sub-map filter (CLSF) technique (Williams, et al., 2002). More specifically, this paper analyses the UHS performance improvement using different Scheduling of the application on CLSF. Some aspects of sensor fusion were considered as well (Sasiadek, 2002).

2 CONSTRAINED LOCAL SUB-MAP FILTER

Constrained Local Sub-Map Filter (CLSF) is a technique to fuse a local map to a global map. A local map can be estimated using FastSLAM into the whole picture of features in the environment previously estimated by UKF. This technique updates the full covariance matrix of the system generated by UKF to be scheduled at "appropriate intervals" (Williams, et al., 2002) defined by FastSLAM based on Rao-Blackwellised Particle Filter (RBPF) (Doucet, et al., 2000). This method provides an independent, local sub-map estimate of the point features in the environment in a small scale and compares the local map that is statistically sampled by particles (Bailey et al., 2006) with the global map produced by UKF-SLAM algorithm. Previous use of such method resulted in a map with the reduction of uncertainty in EKF-SLAM (Brooks, Bailey, 2009). Instead of using EKF to estimate

global and local maps separately and reducing uncertainty, this approach may be substituted by a combination of RBPF and UKF. The observations are fused to create a local map by FastSLAM referenced to a local frame of reference where its global position is already estimated by UKF (Julier, Uhlmann, 2004). At appropriate intervals, the information contained in the local map is transferred into the global map using formulated constraints between the point landmark estimates. The constraint would produce a map of the environment and an estimated path that are identical to the ones previously estimated by UKF. When the vehicle is at location $\mathbf{x}_k^R$ at time step k, a new frame of reference is initiated (Negenborn, 2003). At this moment, the path up to and including time step k is already estimated in the same frame of reference with respect to the global frame of reference and with its minimum uncertainty (assuming it is zero). At the same time step, the global local frame is initialized under UKF calculation. However, the estimation in the local frame of reference by RBPF is completely independent of the estimation that is already done by UKF in the Global frame of reference (Monjazeb et al., 2012). At this time step, only a small state covariance matrix of the system in the global frame of reference is updated with the new observation. Prior to the beginning of time step k+1, the key is switched off to produce a fused map with minimum uncertainty in the system. Once again, at the beginning of time step k+1, the switch turns on to send a local map and to fuse it into the global map estimated by UKF to initiate the process of generating a new global map (Monjazeb et al., 2011).

3 SCHEDULINGS TECHNIQUES

The Unscented HybridSLAM algorithm is arranged in such way so that UKF-SLAM estimates the whole map of the environment and the RBPF estimates the path and the local map in the vicinity of the current robot position (Lijun, et al., 2011). At the CLSF part, there will be an update only on features that are observed in the current local frame of reference (Lindemann, et al., 2006), and the remaining map information will be untouched (Norgard et al., 2000). When the information in the local map is fused into the global map (Sasiadek, Hartana, 2000), the resulting map is replaced with the map in the previous time step. There are two distinct state estimates independent from each other (Neira,

Tardos, 2001), and as a result, the augmented form of posterior state in the process of map fusion can be expressed as

$$\hat{\mathbf{x}}_{k\ (\text{CLSF})}^+ = \{^G\hat{\mathbf{x}}_{k\ (\text{robot})}^+,\ ^G\mathbf{m},\ ^L\hat{\mathbf{x}}_{k\ (\text{robot})}^+,\ ^L\mathbf{m}\} \qquad (1)$$

where, $^G\hat{\mathbf{x}}_{k\ (\text{robot})}^+$ is the global posterior position of the robot estimated by UKF, $^L\hat{\mathbf{x}}_{k\ (\text{robot})}^+$ is the local posterior position of the robot estimated by RBPF, $^G\mathbf{m}$ is the map of landmarks estimated by UKF and $^L\mathbf{m}$ is the map of landmarks in the vicinity of the robot's pose only and estimated by RBPF. The system covariance is defined as

$$\mathbf{P}_k^+ = \begin{bmatrix} ^G\mathbf{P}_k^+ & 0 \\ 0 & ^L\mathbf{P}_k^+ \end{bmatrix} \qquad (2)$$

$$^G\mathbf{P}_k^+ = \begin{bmatrix} ^G_{LL}\mathbf{P}_k^+ & ^G_{mL}\mathbf{P}_k^+ \\ ^G_{mL}\mathbf{P}_k^+ & ^G_{mm}\mathbf{P}_k^+ \end{bmatrix} \qquad (3)$$

$$^L\mathbf{P}_k^+ = \begin{bmatrix} ^L_{RR}\mathbf{P}_k^+ & ^L_{Rm}\mathbf{P}_k^+ \\ ^L_{mR}\mathbf{P}_k^+ & ^L_{mm}\mathbf{P}_k^+ \end{bmatrix} \qquad (4)$$

$^L_{RR}\mathbf{P}_k^+$ is the robot covariance in the local frame of reference, $^L_{mm}\mathbf{P}_k^+$ indicates covariance in the local frame of reference related to landmarks, $^L_{Rm}\mathbf{P}_k^+$ and $^L_{mR}\mathbf{P}_k^+$ represent covariance on robots and landmarks in the local frame of reference as well. $^G_{mL}\mathbf{P}_k^+$, $^G_{mL}\mathbf{P}_k^+$, and $^G_{mm}\mathbf{P}_k^+$ represent same covariance matrices as above but in the global frame of reference. Finally, $^G_{LL}\mathbf{P}_k^+$ is the covariance of the estimate of the local frame of reference with respect to the global frame of reference. In this approach, the position of the robot and the map in the vicinity of the robot position is estimated using particle filters. The resulted data is converted to a single Gaussian and by the use of CLSF the estimated local map is fused to the Global map previously estimated by UKF (Sasiadek et al., 2008). The position of the robot estimated by RBPF in the local map is considered to be as an additional landmark (Thrun, 2000). When the local map covariance matrix is fused to the global map, the related data stays in the main covariance matrix until the next time step (Thrun, et al., 2003).

Figure 1 illustrates a block diagram of the sub-mapping strategy using RBPF, UKF, and CLSF. The strategy in this scheduling is to give the posterior sate of the system at time step k (previously

estimated by RBPF) to the UKF algorithm in order to make an individual map of the environment (the global map). The local map estimated by RBPF is partially used to make an estimation of the path. This local map is then added to the CLSF algorithm, where it is matched with the global map previously estimated by UKF. A new map will be generated based on CLSF algorithm to moment-match the features estimated by each individual algorithm; UKF and RBPF.
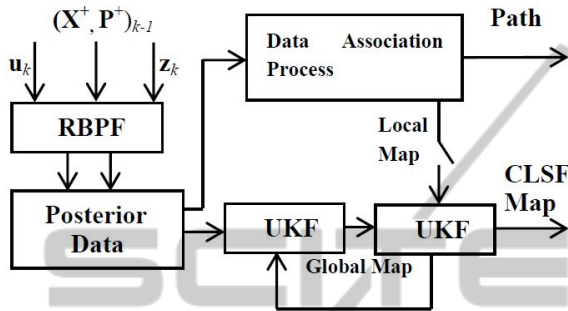
Figure 1: Scheduling without data association incorporation in UKF.
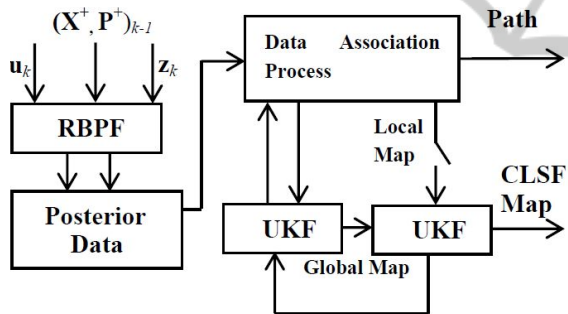
Figure 2: Scheduling with data association incorporation in UKF.

A modified scheduling technique is presented as depicted in figure 2. Instead of updating the global map using a straight forward mean, the ambiguity of the data association is reduced using a data association process algorithm to reduce a cluster of information (Bar-Shalom, Fortmann, 1998). The UKF is then using this modified posterior to generate the global map. The rest of the process is the same as what explained in figure 1. The main difficulty in the mapping process would be to add new landmarks into the map when global and local maps are matched by CLSF. There is a need for a proper formulation in order to make the mapping process reliable (Guivant, Nebot, 2001). If a specific measurement is insufficient to constrain the new landmark in all dimensions, the decision to add a new landmark could be quite challenging. In Kalman-based algorithms, only a single measurement is made to initialize a new landmark. In the RBPF, each observation may be represented in a Gaussian form (Montemerlo, Thrun, 2003) as:

$$\mathbf{z}_k \sim N(\hat{\mathbf{z}}_k + \Lambda_k (\mathbf{z}_{k,i} - {}^n \mu_{k-1,i}), \mathbf{R}_k) \quad (5)$$

This Gaussian can be written as

$$\frac{1}{\sqrt{|2\pi\widetilde{Z}_{k,i}|}} \exp[A . B] \quad (6)$$

$$A = -\frac{1}{2}(\mathbf{z}_k - \hat{\mathbf{z}}_k - \Lambda_k (\mathbf{z}_{k,i} - {}^n \mu_{k-1,i}))^T \quad (7)$$

$$B = \mathbf{R}_k^{-1}(\mathbf{z}_k - \hat{\mathbf{z}}_k - \Lambda_k (\mathbf{z}_{k,i} - {}^n \mu_{k-1,i})) \quad (8)$$

Q is defined as a function equal to the negative of the exponent of this Gaussian:

$$\mathbf{Q} = \frac{1}{2} C . D \quad (9)$$

$$C = (\mathbf{z}_k - \hat{\mathbf{z}}_k - \Lambda_k (\mathbf{z}_{k,i} - {}^n \mu_{k-1,i}))^T \quad (10)$$

$$D = \mathbf{R}_k^{-1}(\mathbf{z}_k - \hat{\mathbf{z}}_k - \Lambda_k (\mathbf{z}_{k,i} - {}^n \mu_{k-1,i}) \quad (11)$$

The second derivative of $\mathbf{Q}$ with respect to $\mathbf{z}_{k,i}$ will be the inverse of the covariance matrix of the Gaussian in landmark coordinates.

$$\frac{\partial Q}{\partial z_{k,i}} = -(\alpha_k - \hat{\mathbf{z}}_k - \Lambda_k (\mathbf{z}_{k,i} - {}^n \mu_{k-1,i})^T \mathbf{R}_k^{-1} \quad (12)$$

$$\Lambda_k$$

$$\frac{\partial^2 Q}{\partial z_{k,i}^2} = \Lambda_k^T \mathbf{R}_k^{-1} \Lambda_k \quad (13)$$

As a result, an invertible observation can be used to create a new landmark as

$${}^n \mu_{k-1,i} = h^{-1}({}^n \mathbf{x}_k^R, \mathbf{z}_k) \quad (14)$$

$${}^n \Sigma_{k,i} = \Lambda_k^T \mathbf{R}_k^{-1} \Lambda_k \quad (15)$$

$${}^n \hat{w}_k = P_0 \quad (16)$$

The initialization of landmarks may be calculated through a simpler formulation. By setting the variance of each landmark parameter to a high value and incorporating the initial observation, the exact initial covariance does not have to be considered. Higher KG values lead the process to a more accurate approximation regarding the observation of each landmark (Thrun et al, 2000).

$$^{n}\mu_{k-1,i} = h^{-1}(^{n}\mathbf{x}_{k}^{R}, \mathbf{z}_{k}) \tag{17}$$

$$^{n}\Sigma_{k,i} = \mathbf{K}\,\mathbf{I} \tag{18}$$

4 SIMULATIONS AND RESULTS

Figure 3 illustrates specifications and dimensions of the vehicle defined as A=3.00m, ℓ=2.00m, W=0.70m, and B=0.2m. Speed of the vehicle is assumed to be a constant but changing from 1m/s to 5m/s in different scenarios.
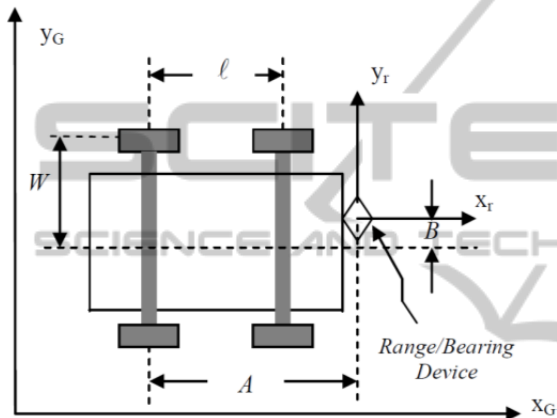
Figure 3: Mobile robot dimensions.

The vehicle is equipped with a range/bearing finder device and capable of detecting 100 visible landmarks in the environment. The maximum range defined for the range/bearing device is assumed 40.00m. An encoder attached to the vehicle's rear tire measures its revolutions and infers the linear displacement. An accelerometer is also used to measure the change in heading. A combination of heading and displacement measurements is incorporated into the UHS algorithm in order to dead reckon the vehicle location in the global frame of reference. Figure 4 depicts a situation in which the autonomous robot is travelling in a 100m by 100m environment with a speed of 1m/s.

In order to compare two different scheduling techniques, the RMS position error is depicted for each situation. Figure 5 demonstrates the error in the situation in which the data association is not incorporated into the UKF map calculation. The error in this case exceeds up to 0.5m. In figure 6, the RMS position error fluctuations do not show much of a difference if the data association process interferes with the UKF map calculation. However, the process time increases slightly (around 150s)

which indicates that adding the data association calculation into UKF map building has its effect on the process. Figures 7 and 8 depict the average orientation error for both cases demonstrated in figures 5 and 6. Results show that the error stays at the same level (around 0.03rad) when the speed of the vehicle is around 1m/s. It should be mentioned that the system function that describes the concurrent mapping of the environment is highly non-linear. Furthermore, perturbations of the system are quite hard to control due to a noisy measurement. The significant amount of system noise, affects the accuracy of map estimation process. In real world applications, it is fair to assume that both absolute and relative measurements are functions of vehicle speed. As a result, the faster the vehicle moves, the less accuracy is expected.
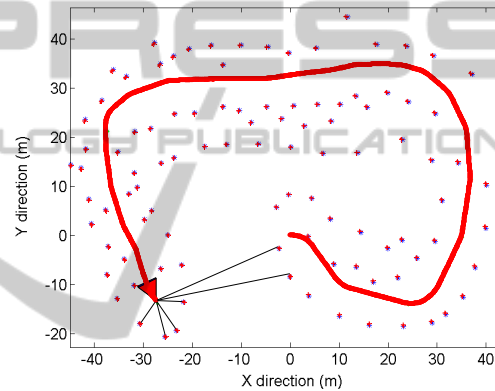
Figure 4: Autonomous robot travelling in a 100m×100m square environment.
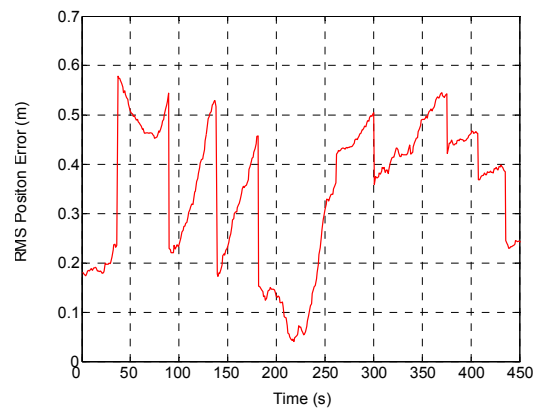
Figure 5: RMS position error for UKF mapping without data association scheduling for v=1m/s.

To further investigate the effect of data association calculation on the mapping process, the speed of the vehicle is set to 5m/s and the UKF mapping calculation is done with and without influence of the

data association process. The average RMS position error stays around 0.6m. The error is relatively increased compared to the situation in which the speed is 1m/s. It is expected to have such increase in error because the accuracy of raw sensor data extraction and converting it to lower dimensional feature vector highly depends on the speed of the vehicle which in turn, affects the accuracy of the perception process. Figure 9 shows such increase in error when the speed changes from 1m/s to 5m/s. However, the increase in RMS position error is not as much when the data association calculation is influences the UKF mapping process. Figure 10 shows that as long as the UKF mapping stage takes advantage of the data association process, the change in speed would not affect the map accuracy.
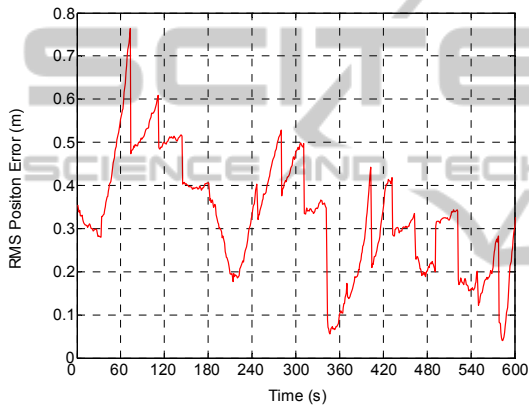
Figure 6: RMS position error for UKF mapping with data association scheduling for v=1m/s.
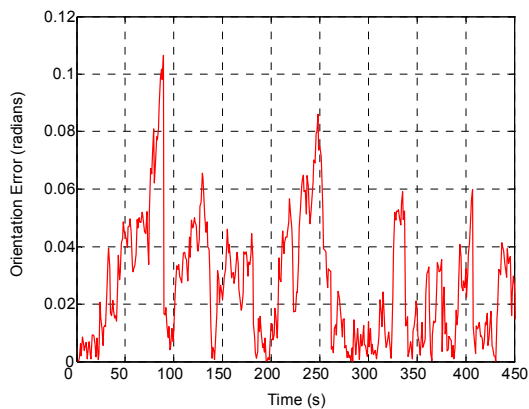
Figure 7: Orientation error for UKF mapping without data association scheduling for v=1m/s.

The process time, however, increases substantially which indicates that the mapping process is consuming more than regular time when the data association is processed in the UKF algorithm. The same result is inferred from figures 11 and 12 in terms of the orientation error. The orientation error is not as much increased when the data association process interfere the UKF mapping calculation once the speed of the vehicle is increased to 5m/s.
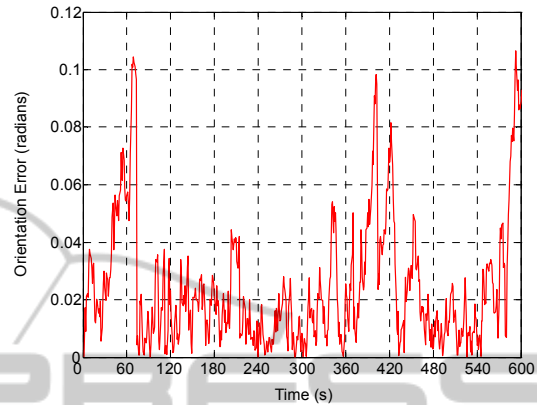
Figure 8: Orientation error for UKF mapping with data association scheduling for v=1m/s.

One of the major reasons that the process time increases is the computational power that is needed to extract a real time image. Nowadays, current CPUs are quite fast but not fast enough to provide processing power for a real time application. Depending on how much the data associated with landmarks is incorporated into the map estimation process, the demanding processing power for data extraction varies. At a reasonable cost, a compromise between the processing power and a real time image must be considered.
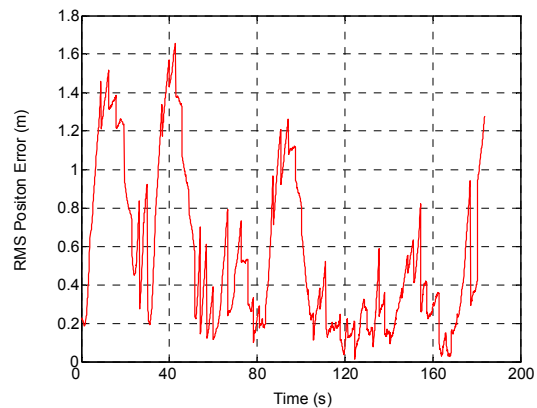
Figure 9: RMS position error for UKF mapping without data association scheduling for v=5m/s.

A number of runs were performed and the UKF estimated the global map at different speed. Figures 13 and 14 depict resulting RMS position error and

orientation error for two different scheduling. The vehicle speed changes from 1m/s to 10m/s. As illustrated in these figures, the error increases for both scheduling techniques as the vehicle speed increases. Ideally, at a low speed basis, the error stays at the same level. Once the speed increases, the performance of UKF with data association calculation varies from the situation in which the data association process does not influence the global mapping estimation. At the speed of 5m/s there is a substantial difference between two techniques and this difference even grows at higher speed sets. In practical situations, those scheduling techniques may not always reflect the ideal condition as plotted in figures 13 and 14. Other factors such as system noise or device failures may play major roles in the performance of the algorithm.

process time versus vehicle speed for both scheduling techniques. Again, in low speed conditions the effect of data association process on the process time is negligible but as the vehicle speed is added up, the process time increases substantially. For relatively high speed situations, the scheduling technique with the data association influence in global mapping becomes nuisance even though the error stays at a reasonable level. It should be noted that one of the main intentions in a scheduling technique is to bring the system enough accuracy in estimation of the map and as close to real time as possible. In order to achieve these goals, an optimal point must be selected for each scheduling technique. From figures 13 to 15 and for this particular platform the map estimation influences the UKF map calculation and with speed set to 4m/s is the closest to the desired condition.
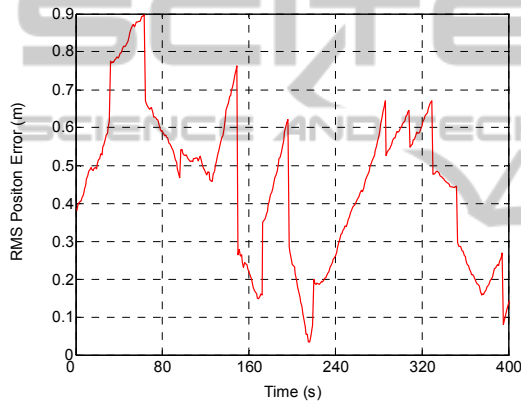
Figure 10: RMS position error for UKF mapping with data association scheduling for v=5m/s.
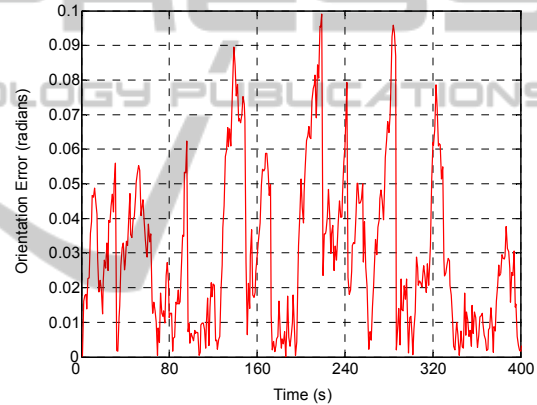
Figure 12: Orientation error for UKF mapping with data association scheduling for v=5m/s.
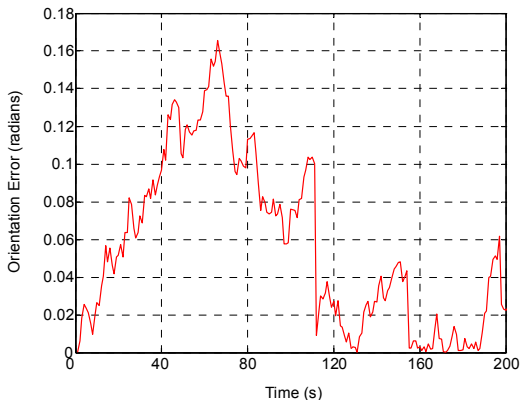
Figure 11: Orientation error for UKF mapping without data association scheduling for v=5m/s.

Nevertheless, the deterioration rate stays similar to the ideal condition, meaning that, the higher the vehicle speed is set to, the more erroneous estimation is resulted. Figure 15 illustrates the
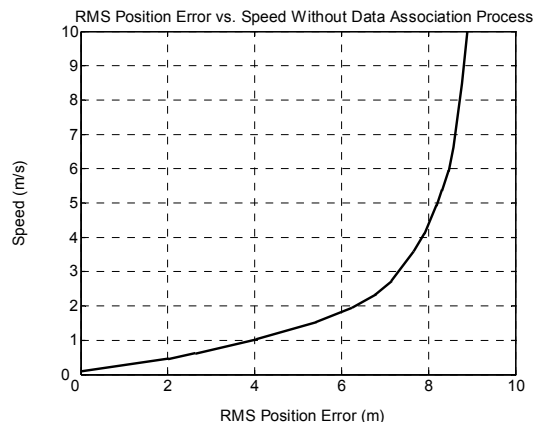
Figure 13: RMS position error for global map estimation without data association technique for v=1m/s to 10m/s.

It is interesting that the divergence between two scheduling techniques occurs around 2m/s. This

indicates that as long as the vehicle speed is maintained around 2m/s, there is no need to use the scheduling in the global map estimation by UKF.
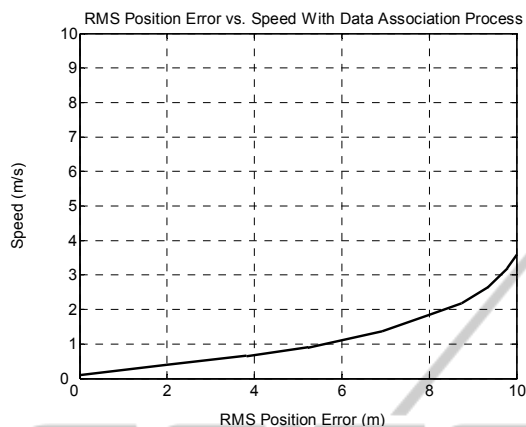
Figure 14: RMS position error for global map estimation with data association technique for v=1m/s to 10m/s.
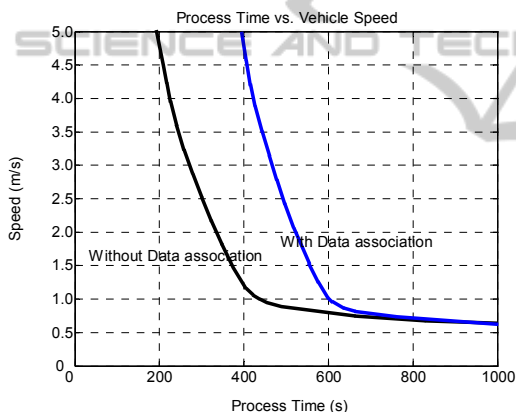
Figure 15: Computing time versus vehicle speed for different scheduling techniques.

Once a specific combination of map accuracy and process time is desired, depending on the application, one can extract different variances of the speed, time, and map accuracy. It is also evident that for high speed settings, the data association scheduling in the UKF map estimation process causes an exponential increase in the process time.

5 CONCLUSION

In this paper, two different scheduling techniques were briefly discussed and several mapping scenarios were simulated via MATLAB and C++ codes for an autonomous robotic vehicle to map the environment. The map accuracy through both different techniques and in different settings was discussed. Variations of each technique were demonstrated in terms of Root Mean Square position error and orientation error. In order to formalize the mapping calculation, a data association process was defined and applied for the global mapping estimation using Unscented Kalman Filter. It was concluded that depending on the application and in order to get the best result, a compromise between the process time and map accuracy is necessary. In this particular scenario and for the specific platform used in this study, the scheduling technique can be used in global mapping estimation. The speed of the vehicle in this case was set between 2m/s to 4m/s. It was also concluded that for a desired accuracy, there will be an unavoidable increase in the computing time that is negligible for low speed settings. However, if a shorter computing time is desired, a decrease in vehicle speed setting is required.

ACKNOWLEDGEMENTS

REFERENCES

Durrant-Whyte H., Bailey T., 2006, Simultaneous localization and mapping (SLAM): part I the essential algorithms, *IEEE Robatics and Automation Magazine*, Vol. 13, No. 2, pp. 99-108, June.

Smith R., Cheeseman P., 1986, The estimation and representation of spatial uncertainty, *International Journal of Robotics Research*, Vol. 5, Issue 4, pp. 56-68.

Jaulin L., 2011, Range-only SLAM with occupancy maps: A set-membership approach, *IEEE Transaction on Robotics*, Vol. 27, Issue 5, pp. 1004-1010, May 31st.

Monjazeb A., Sasiadek J. Z., Necsulescu D., 2013, Autonomous robot positioning using Unscented HybridSLAM, *Proc. International Conference on Methods and Models in Automation and Robotics (MMAR)*, pp. 588 – 593, Miedzyzdroje, Poland, 28-31 August.

Julier S. J., Uhlmann J. K., 2001, A counter example to the theory of simultaneous localization and map building, *Proc. of IEEE International Conference on Robotics and Automation*, pp. 4238-4243, March.

Montemerlo M., Thrun S., Koller D., Wegbreit B., 2002, "FastSLAM: A factored solution to the simultaneous

localization and mapping problem", *Proceedings of AAAI National Conference of Artificial Intelligence.*

Brooks A., Bailey T., 2009, HybridSLAM: Combining FastSLAM and EKF-SLAM for reliable mapping, *Springer Tracts in Advanced Robotics*, Volume 57, pp. 647-661.

Williams S. B., Dissanayake G., Durrant-Whyte H., 2002, An Efficient Approach to the Simultaneous Localisation and Mapping Problem, *Proceedings of the IEEE International Conference on Robotics & Automation*, Washington DC.

Sasiadek, J. Z., 2002, Sensor Fusion, Annual Reviews in Control, *IFAC Journal*, pp. 203-228, No. 26.

Doucet A., Freitas N., Murphy K., Russell S., 2000, Rao-Blackwellised particle filtering for dynamic Bayesian Networks, *Proceedings of Conference on Uncertainty in Artificial Intelligence.*

Bailey T., Nieto J., Nebot E., 2006, Consistency of FastSLAM algorithm, *Proceedings of IEEE International Conference on Digital Object Identifier*, pp. 424-429.

Julier S. J., Uhlmann J. K., 2004, Unscented filtering and nonlinear estimation, *Proc. of IEEE Journal*, Vol. 92, Issue 3, pp. 401-422, March.

Negenborn R., 2003, Robot localization and Kalman filters: on finding your position in a noisy world. MSc. Thesis, Utrecht University, Netherland.

Monjazeb A., Sasiadek J. Z., Necsulescu D., 2012, An approach to autonomous navigation based on Unscented HybridSLAM, *Proc. of 17th International Conference on Methods and Models in Automation and Robotics*, pp. 369-374, Miedzyzdroje, Poland.

Monjazeb A., Sasiadek J. Z., Necsulescu D., 2011, Autonomous navigation among large number of nearby landmarks using FastSLAM and EKF-SLAM; a comparative study, *Proc. of 16th International Conference on Methods and Models in Automation and Robotics (MMAR)*, pp. 369-374, Miedzyzdroje, Poland.

Lijun Z., Lianzheng G., Ke W., Ruifeng L., 2011, A Hybrid SLAM method for service robots in Indoor Environment, *Proceedings of 30th Chinese Control Conference (CCC)*, pp. 4034-4039, Yantai, China, July.

Lindemann R. A. , Bickler D. B., Harrington B. D., Ortiz G. M., Voothees C. J., 2006, Mars exploration rover mobility development, *IEEE Robotics and Automation Magazine*, pp. 19-26, Vol. 13, Issue 2.

Norgard M., Poulsen N., Ravn O., 2000, New development in state estimation for nonlinear systems, *IFAC Automatica*, pp. 1627-1638, Vol. 36, No. 11, November.

Sasiadek J. Z., Hartana P., 2000, Odometery and sensor data fusion for mobile robot navigation, Proceedings of the *6th IFAC Symposium on Robot Control*, pp. 531-536, SYROCO.

Neira J., Tardos J., 2001, Data association in stochastic mapping using the joint compatibility test, *IEEE Transactions on Robotics and Automation*, pp. 890–897, Vol. 17.

Sasiadek J. Z., Monjazeb A., Necsulescu D., 2008, Navigation of an autonomous mobile robot using EKF-SLAM and FastSLAM, *Proc. of 16th Mediterranean Conference on Control and Automation*, pp. 517-522, Ajaccio, France.

Thrun S., 2000, Probabilistic algorithms in robotics, *AI Magazine 21*, 4, pp. 93- 109.

Thrun S., Ferguson D., Haehnel D., Montemerlo M., Burgard W., Triebel R., 2003, A system for volumetric robotic mapping of abandoned mines, *Proceedings of the IEEE International Conference on Robotics and Automation (ICRA'03)*.

Bar-Shalom Y., Fortmann T., 1998, Tracking and data association, *Academic press*, Inc.

Guivant J., Nebot E., 2001, Optimization of the simultaneous localization and map building algorithm for real time implementation, *IEEE Transactions on Robotics and Automation*, 17(3):242–257.

Montemerlo M., Thrun S., 2003, Simultaneous localization and mapping with unknown data association using FastSLAM, *Proceedings of the IEEE International Conference on Robotics and Automation*, pp. 1985-1991, Vol. 2, September.

Thrun S., Fox D., Burgard W., 2000, Monte Carlo Localization with mixture proposal distribution, *Proceedings of AAAI National Conference on Artificial Intelligence*, Austin, Texas, USA.